Vol. 35, No. 1 (2013) 74-83

Tribology in Industry

www.tribology.fink.rs

RESEARCH

The Effect of Compression Ring Profile on the Friction Force in an Internal Combustion Engine

A. Sonthalia[a], C.R. Kumar[a]

[a]*VIT University, India.*

Keywords:

Friction
Ring profile design
Simulation
Floating liner method

Corresponding author:

C. Ramesh Kumar
VIT University, India
E-mail: crameshkumar@vit.ac.in

A B S T R A C T

In an internal combustion engine piston, piston ring and cylinder are the most important assembly for transmitting the forces produced by the combustion process. The friction between piston ring pack and cylinder accounts for major portion of friction in an internal combustion engine and it also significantly affects the mechanical efficiency of the engine. In the piston ring pack, friction is mainly due to the compression ring, especially at the top dead centre and bottom dead centre where boundary lubrication exists. This paper provides a detailed study on the effect of ring profile on ring friction using MATLAB code. Three different ring profiles were selected and analysed for lubricant film thickness, ring twist angle, ring friction and friction coefficient. Out of these three, friction force and friction coefficient of one ring profile design was found minimum. The ring design with minimum friction force and friction coefficient was manufactured and assembled in a low speed SI engine. The engine liner was modified to float and friction of the ring was studied using motoring test method. The experimental results were compared with the simulation result, it was found that simulation result was in agreement with the experimental result.

1. INTRODUCTION

Reducing fuel consumption in IC engine is important from viewpoints of both effective use of oil resources and prevention of global warming. For realizing a better heat balance in engines it is desirable that not only combustion efficiency but also mechanical efficiency is improved. Reduction of friction loss is a proper measure of the improvement in mechanical efficiency as pointed out by many engine developers and researchers [1]. 30-50 % of total friction losses in an internal combustion engine occur at the interfaces of piston cylinder, piston ring-cylinder, and piston-piston ring. Even small reduction in friction at piston ring-cylinder liner interface may contribute in significant fuel saving and reduction in emissions [2,3]. The piston rings move freely in its grooves and these movements depends on the forces acting on the piston ring system, like, the ring tension due to the placement of the piston ring in cylinder, the gas pressure forces due to combustion and blow-by, the hydrodynamic force due to lubricant film, the inertia forces due to the ring mass, the engine speed and asperity contact

forces between the ring and cylinder walls [4]. The study of piston ring motion leads to a better understanding of these mechanisms and many researchers have attempted to understand the same through experimental studies. For example, the investigation of the friction force exerting on the piston ring using floating liner test rig [5], and the investigation of oil film thickness was done using ultraviolet light [6] and using differential voltage drop method [7].

Similarly, piston ring motions have also been studied, through simulation method [6-10]. The model used by these researchers were similar for each mechanism, but with different procedures and assumptions. However, they did not revealed the detailed steps of simulation.

The present work aims to analytically study the effect of piston ring profile on the friction force. Three different ring profiles were analyzed for lubricant film thickness, ring twist angle, ring friction and friction coefficient using the MATLAB code. The ring with the minimum friction force was manufactured and tested using non firing floating liner method. The friction force computed from the theoretical analysis was compared with the experimental results.

2. THEORETICAL ANALYSIS OF PISTON RING

Initially, the dimensionless parameters that characterize the operation of a piston ring and its friction were identified. Next an analytical model describing the dynamics surrounding ring's performance was developed. Using this model in numerical simulation, the operational behavior of ring was predicted. The in-cylinder pressure which is one of the inputs for the MATLAB code was simulated using the first law of thermodynamics.

2.1 Assumptions

The following assumptions were considered for the analytical model:

Side thrust force is the largest cause of friction in an internal combustion engine, this force is transmitted to the cylinder wall on the thrust side, resulting in noticeable wear on the wall near the top dead centre position of first ring. This force is neglected in this work since our focus in only on interaction between ring, the piston and the wall. The ring is much wider in its relaxed state but when installed in the cylinder the ring was squeezed to fit in the cylinder.

The ring deflects inwards and it exerts a local elastic pressure on the cylinder wall. In this study it is assumed that the ring contracts and expands equally round the circumference. It was assumed that the ring rests on a single point, as shown in Fig. 1, with a rolling contact on the topland or the bottomland of the groove. The angle of tilt is used to determine the contact point. It is assumed that the contact points seal the pressure on one side from the other so that there is a step change in the pressure across this contact point. Due to reciprocating motion of the piston in the cylinder, the velocity of the piston is maximum at the mid-stroke and zero at the dead centers.

The change in piston speed changes the lubrication regime in the cylinder, which in turn changes the friction between the ring and the liner during the entire stroke of the piston. The frictional patterns which the piston ring would experience can be classified into different modes based on this lubrication regime [11]. In this study hydrodynamic lubrication was assumed i.e. the ring always rides on full fluid film.

The friction force peaks at the midpoint, where the speed is at its maximum, i.e. it is proportional to the instantaneous piston speed in mid-stroke. If the engine speed or oil viscosity is high, a thick oil film is formed that would not be completely squeezed out even at dead centers where the piston velocity falls to zero [11]. Also, the effect of temperature on oil viscosity was not considered. Using these assumptions a model for theoretical analysis of piston rings was made using cosine method [12] and the governing equations were solved by bisection method.

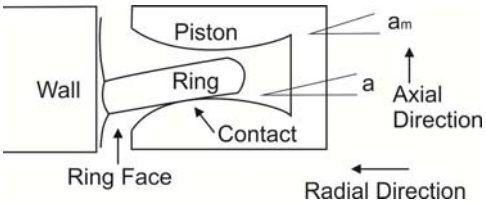

Fig. 1. Ring pivot position.

2.2 The governing equations

The Reynolds' equation [13], for a fully lubricated gap; which indicates the relationship the pressure and film shape as a function of viscosity and velocity, can be used, which is given by (1).

$$\frac{\partial}{\partial x}\left(h^3\frac{\partial P}{\partial x}\right)+\frac{\partial}{\partial y}\left(h^3\frac{\partial P}{\partial y}\right)=6U\eta\frac{dh}{dx}+6V\eta\frac{dh}{dy}+12\eta\frac{dh}{dt} \quad (1)$$

Assuming axis symmetry along the cylinder axis, at each instant of time [1] can be written in one dimensional form for piston and ring liner contact:

$$\frac{\partial}{\partial x}\left(h^3\frac{\partial P}{\partial x}\right)=6U\eta\frac{dh}{dx}+12\eta\frac{dh}{dt} \quad (2)$$

To produce pressure in the oil film, the film thickness under the ring changes with respect to time, is given by (3)

$$h(x,t)=h_p(x)+h_r(t)+a(t).x \quad (3)$$

Using classical slit flow theory, the shear stress between two parallel plates is given by Eq.4

$$Shear=\frac{h}{2}\frac{\partial P}{\partial x}-\frac{\eta U}{h} \quad (4)$$

The piston ring in the piston fits loosely in the ring groove, thus leaving room axially and behind the ring. Due to this the ring can move axially in its groove, from topland to bottomland, depending upon operating conditions [12]. It can thus be assumed that ring operates in two modes (Fig. 2) it is either on topland or bottomland. The ring can be considered a free body which is influenced by outside forces: On the front surface, there is a normal oil pressure distributed over the axial width, which produces a normal force as well as a moment on the ring surface. When the ring is resting on the bottomland, the pressure above and behind the ring is assumed to be the combustion chamber pressure (Fig. 3). However, the pressure below is the crankcase pressure and the combustion pressure before the contact point thus a step in pressure can be seen in Fig. 3.

On the other hand when the ring is resting on topland the pressure step is on the top surface and the pressure behind and below the ring is assumed to be same as that of the crankcase. The elastic properties of the ring also exert an effective elastic pressure on the ring in radial direction. The inertial properties of the ring exerts a d' Alembert force axially on the ring, as it is moving along with the piston.

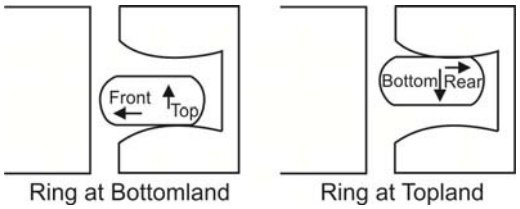

Fig. 2. Ring modes.

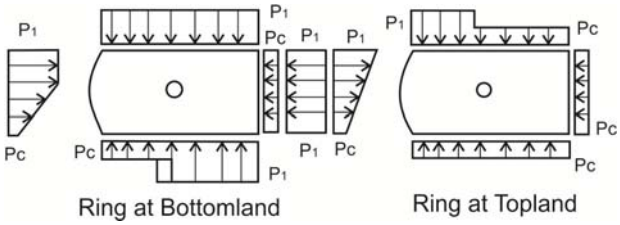

Fig. 3. Pressure distributions about ring.

Composite Secant method [12] was used to find the ring friction, ring twist angle and the film height. The above equations were normalized, and then a MATLAB code was written to find the effects of ring movement in the cylinder liner.

The normalized equations are given below.

The dimensionless radial force acting on the ring is given by [5].

$$F_1=-1-\frac{\Delta P}{P_e}+\frac{6U\eta L_1}{P_e W\bar{h}^2}\frac{1}{h_r'}\left[\left[\frac{L_2}{L_1}\right]^2\frac{1}{z_2^2}\left(\frac{z_2^2}{4}+\frac{\sin^2 z_2}{4}-\right.\right.$$
$$-\frac{\sec\bar{\theta}}{3}\left(\frac{\sin^2 z_2}{2}-2\cos z_2+2\right)+C_2 z_2\Big)-$$
$$\left.-\frac{1}{z_1^2}\left(\frac{z_1^2}{4}+\frac{\sin^2 z_1}{4}-\frac{\sec\bar{\theta}}{3}\left(\frac{\sin^2 z_1}{2}-2\cos z_1+2\right)+C_1 z_1\right)\right] \quad (5)$$

The dimensionless moment equation for the oil is given by [6].

$$F_2 = \left(\frac{\Delta P_1 B^2}{4P_e W^2}\right)\left(1-\frac{\alpha'}{\alpha_0'}\right)+\frac{\Delta P}{P_e}+1-\frac{EBW\bar{\alpha}\alpha'}{6P_e R_{cyl}^2}-$$
$$\frac{\rho B^2 Y\bar{\alpha}}{P_e W\alpha_m}+\left(\frac{U\eta L_1 B}{P_e W^2\bar{h}}\right)\frac{1}{h_r'}\left[\frac{\sin z_1}{z_1}+\left(\frac{L_2}{L_1}\right)\frac{\sin z_2}{z_2}+\right.$$
$$\frac{3}{z_1}\left(\sin z_1 - z_1\frac{\sec\bar{\theta}}{2}-\frac{\sec\bar{\theta}}{4}\sin 2z_1\right)-$$
$$\left.\frac{3}{z_2}\left(\frac{L_2}{L_1}\right)^3\left(\sin z_2 - z_2\frac{\sec\bar{\theta}}{2}-\frac{\sec\bar{\theta}}{4}\sin 2z_2\right)\right]-$$
$$\left(\frac{12U\eta L_1^2 L_2}{P_e W^2\bar{h}^2}\right)\frac{1}{h_r'^2}\left\{\left(\frac{L_2}{L_1}\right)^2\frac{1}{z_2^2}\left[\frac{z_2^2}{4}+\frac{\sin^2 z_2}{4}-\right.\right.$$
$$\frac{\sec\bar{\theta}}{3}\left(\frac{\sin^2 z_2}{2}-2\cos z_2+2\right)+C_2 z_2\Big]-$$
$$\frac{1}{z_1}\left[\frac{z_1^2}{4}+\frac{\sin^2 z_1}{4}-\frac{\sec\bar{\theta}}{3}\left(\frac{\sin^2 z_1}{2}-2\cos z_1+2\right)+\right.$$
$$\left.C_1 z_1\right]\Big\}-\left(\frac{12U\eta L_1^3}{P_e W^2\bar{h}^2}\right)\frac{1}{h_r'^2}\left\{\frac{1}{z_1^3}\left[\frac{z_1^3}{6}+\frac{\sin 2z_1}{16}-\right.\right.$$
$$\frac{z_1}{8}\cos 2z_1+\frac{2\sec\bar{\theta}}{3}\left(z_1\cos z_1-\sin z_1-\frac{\sin 2z_1}{16}+\right.$$
$$\left.\left.\frac{z_1}{8}\cos 2z_1+C_1\frac{z_1^2}{2}\right)\right]+\frac{1}{z_2^3}\left(\frac{L_2}{L_1}\right)^3\left[\frac{z_2^3}{6}+\frac{\sin 2z_2}{16}-\right.$$
$$\frac{z_2}{8}\cos 2z_2+\frac{2\sec\bar{\theta}}{3}\left(z_2\cos z_2-\sin z_2-\frac{\sin 2z_2}{16}+\right.$$
$$\left.\left.\left.\frac{z_2}{8}\cos 2z_2+C_2\frac{z_2^2}{2}\right)\right]\right\} \quad (6)$$

The dimensionless axial force is given by [7].

$$F_3 = -\frac{\Delta P_1 B\bar{h}}{2\bar{U}\eta W}\left[1-\frac{\alpha'}{\alpha_0'}\right]-\frac{L_1\sin z_1}{Wz_1 h_r'}-\frac{L_2\sin z_2}{Wz_2 h_r'}-$$
$$\frac{3UL_1}{\bar{U}Wz_1 h_r'}\left(\sin z_1 - z_1\frac{\sec\bar{\theta}}{2}-\frac{\sec\bar{\theta}}{4}\sin 2z_1\right)+ \quad (7)$$
$$\frac{3UL_2}{\bar{U}Wz_2 h_r'}\left(\sin z_2 - z_2\frac{\sec\bar{\theta}}{2}-\frac{\sec\bar{\theta}}{4}\sin 2z_2\right)-$$
$$\frac{\rho Y B\bar{h}}{\bar{U}\eta}$$

C1, C2 and sec $\bar{\theta}$ is given by Eq. 8, 9 and 10 respectively.

$$C_1 = -\frac{\Delta P z_1 h_r}{6U\eta L_1}-\frac{1}{2}+\left(z_1+\sin z_1\cos z_1\right)+ \quad (8)$$
$$\sec\bar{\theta}\sin z_1\left(2+\cos z_1\right)$$

$$C_2 = -\frac{1}{2}\left(z_2+\sin z_2\cos z_2\right)+\sec\bar{\theta}\sin z_2\left(2+\cos z_2\right) \quad (9)$$

$$\sec\bar{\theta} = \frac{\frac{\Delta P_1 h_r^2}{6U\eta}+\frac{W}{2}+\frac{L_1\sin z_1\cos z_1}{2z_1}+\frac{L_2\sin z_2\cos z_2}{2z_2}}{\frac{L_1\sin z_1\left(2+\cos z_1\right)}{3z_1}+\frac{L_2\sin z_2\left(2+\cos z_2\right)}{3z_2}} \quad (10)$$

2.3 Simulation Algorithm

A step wise procedure was used for simulating the piston and piston ring mechanisms at any instant of time during the engine cycle. The ring inclination angle α_1 was assumed initially. α_1 was substituted into the force equation (F_1 (5)) and the film thickness h_{r1} was calculated by the bisection method. α_1 and h_{r1} were then substituted into the moment equation (F_2 (6)) and the residue of F_2 (α_1, h_{r1}) was calculated.

The algorithm then assumes another α_2, and solves for h_{r2}, α_2 and h_{r2} were then substituted into F_2 (6), and the residue of F_2 (α_2, h_{r2}) was calculated. If the residues were of opposite sign, a solution exists between α_1 and α_2. For each crank angle, the values of the state variables α, h_r and the friction was calculated.

2.4 Input for the Program

Simulated cylinder pressure with respect to crank angle was used as input. Three ring profiles were considered, as shown in figure 4 and their profiles were normalized to form two secant curves joined back to back. This shape approximates the ring more closely and its associated oil pressure distribution also resembles the actual moment distribution. The physical and operating properties that are required are given in Table 1. The ring profile properties are given in Table 2.

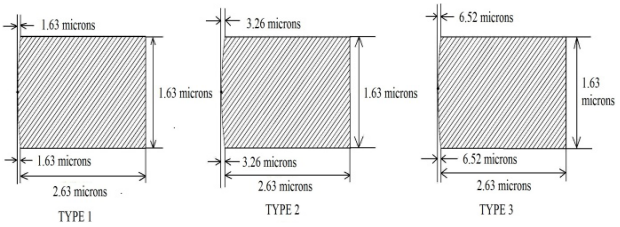

Fig. 4. Different ring profiles.

Table 1. Input parameter for simulation program.

Parameters	Value
Connecting Rod Length	127 mm
Crank Radius	28.7 mm
Ring Axial Width	1.63mm
Ring Radial Width	2.63 mm
Piston Bore Diameter	70 mm
Oil Density	881.5 kg/m^3
Oil Viscosity	0.008736 Pa-s
Ring Density	7900 kg/m^3
Ring Modulus of Elasticity	2.05 e11 Pa
Ring Elastic Pressure	93539 N/m^2
Engine Speed	3000 rpm
Compression Ratio	6.67

Table 2. Ring profile property.

Property	Type I	Type II	Type III
Ring Surface Crest Position	0.5 cm	0.5 cm	0.5 cm
Ring Surface Upper Profile Height	1.63 μm	3.26 μm	6.52 μm
Ring Surface Lower Profile Height	1.63 μm	3.26 μm	6.52 μm

3. EXPERIMENTAL SETUP

A single cylinder 4-stroke spark ignition engine was coupled to a DC motor cum generator on a test rig. Engine specification is given in Table 3.

Table 3. Engine specification.

Parameters	Value
Make	Greaves MK-25
Type	4-stroke, side valve
Engine Capacity	256 cc
Bore	70 mm
Stroke	66.7 mm
Compression Ratio	6.67
Maximum Power	2.5 kW @ 3000 rpm
Maximum Torque	14Nm @ 1700 rpm
Cooling System	Forced Air Cooling
Lubrication	Splash type

Ammeter and voltmeter were used for power measurements. The prime mover, a DC shunt motor, was chosen in order to keep the speed constant and precise without fluctuation. Using a Ward Leonard system the motor was connected and speed was varied from zero to 2000 rpm. Using diodes AC power was converted to DC power to run the prime mover. The tests were performed using non firing condition. A simple sketch shown in Fig. 5 describes the setup of the test rig onto which the engine and motor are being mounted.

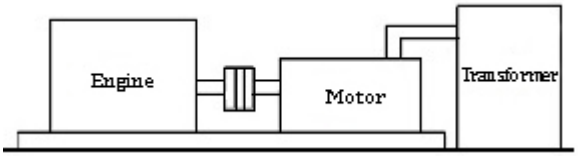

Fig. 5. Test setup.

A simplified floating liner was designed and fabricated for this experiment. The liner was constrained to move only in the vertical direction using the mounting guide studs. A piezoelectric force sensor was mounted on a support stand and it was attached to the liner as shown in Fig. 6. When the piston is moving towards TDC, the rubbing friction between the piston and liner imparts a force which tends to move the liner along with the piston in the vertical direction. The force sensor restricts the movement of the liner and converts the movement into voltage signals. Using a charge amplifier, cathode ray oscilloscope (CRO) and data acquisition system, the voltage signal was transferred to a personal computer. A crank angle encoder was used to measure the crank angle, which gives voltage peaks when the piston reaches the TDC.

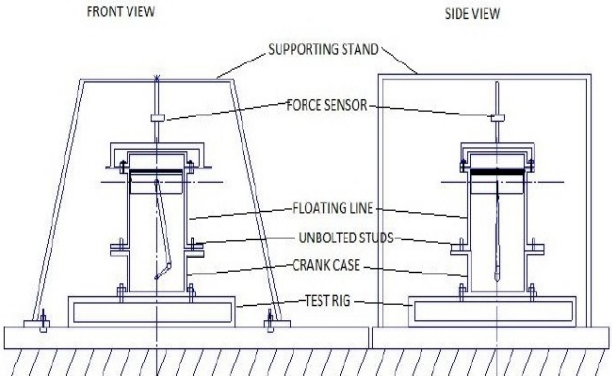

Fig. 6. Test setup.

4. RESULTS AND DISCUSSIONS

The piston position, velocity and acceleration needed for ring dynamics model were found using the piston kinematics equations (Appendix I) and were plotted as shown in Figs. 7-9. Simulated cylinder pressure is shown in figure 10. The piston axial position is considered with

respect to Bottom Dead Centre (BDC) where piston's axial position is zero.

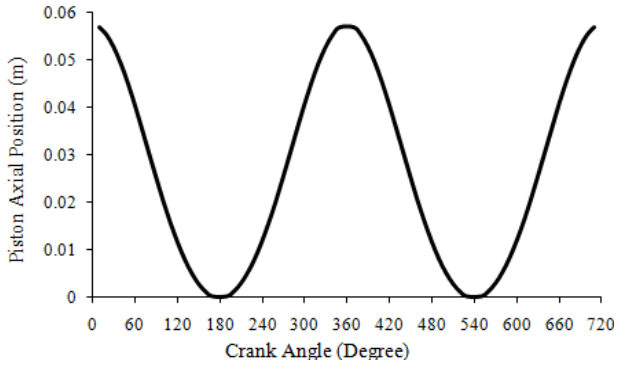

Fig. 7. Piston axial location.

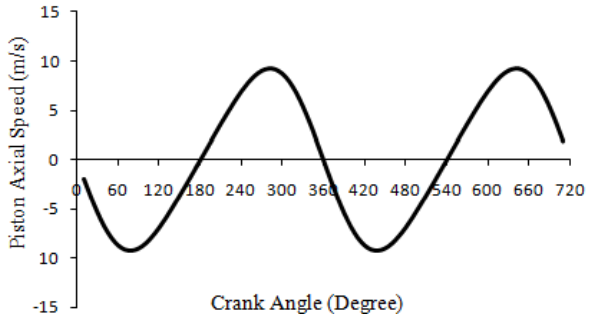

Fig. 8. Piston axial speed.

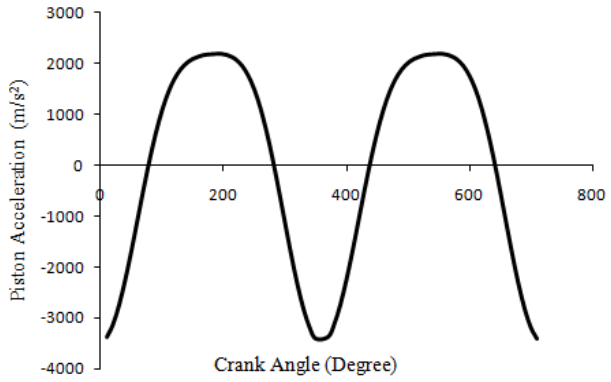

Fig. 9. Piston acceleration.

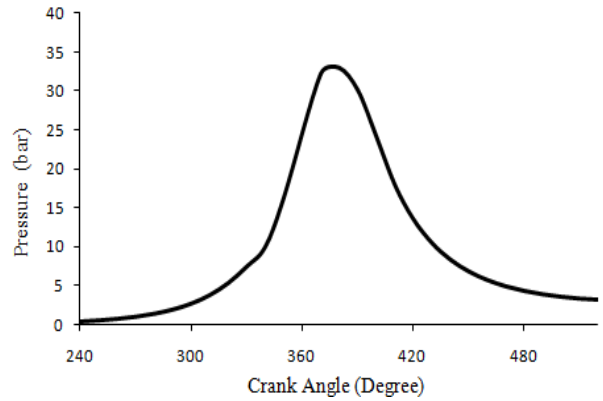

Fig. 10. Simulated cylinder pressure.

The simulated result for non-dimensional ring twist angle is shown in Fig. 11. The positive values of the twist angle refer to the ring's back (inner diameter) moving down and the ring's face moving up. The largest twist will take place just after Top Dead Centre (TDC) following compression, since it is necessary to generate the lift force as the piston speed is low at the TDC. It can be seen that Type 3 has the smallest ring twist angle, and Type 1 having the largest ring twist angle.

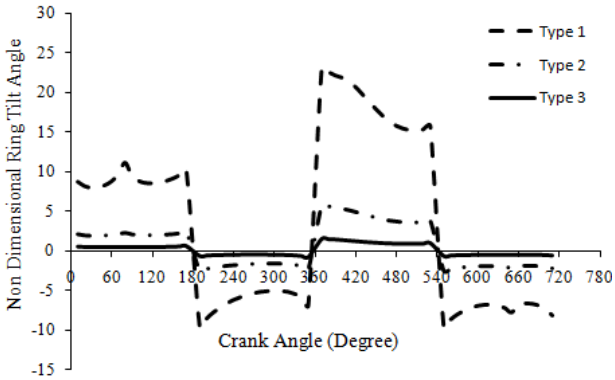

Fig. 11. Ring twist angle.

Figure 12 shows the non-dimensional lubricant film thickness with respect to crank angle. The compression and power stroke has lower film thickness contributing to increase friction. The exhaust stroke is similar to the intake stroke, as the cylinder gas pressure is closer to atmospheric pressure. At both the dead center the film is very thin, especially at the TDC after compression stroke; this may result in heavy wear of the cylinder wall due to surface to surface contact. Type 1 ring profile has highest oil film thickness and type 3 the lowest.

In order to validate the film thickness values obtained through simulation, data collected from literature was utilized, as shown in Fig. 13. Takiguchi et al. [8] conducted experiments on a four- stroke engine and found the film thickness. The same engine parameters were used as input for the MATLAB code to find the oil film thickness. Since some data were not available, few assumptions were made as inputs of the program, like the ring radial width which was assumed to be 0.4 times the bore [15], ring material properties where the ring density was 7600 kg/m^3 and modulus of elasticity was taken to be 1.2e^{+11}. The output of the simulation code is almost matching with the work done by Takiguchi et al. [8]. The

small variations could be due to the assumptions that were made for the input.

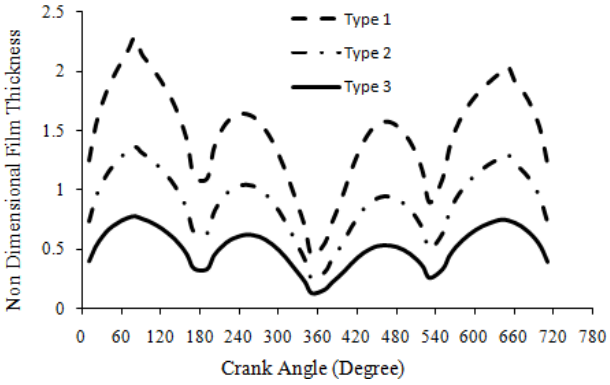

Fig. 12. Lubricant film thickness.

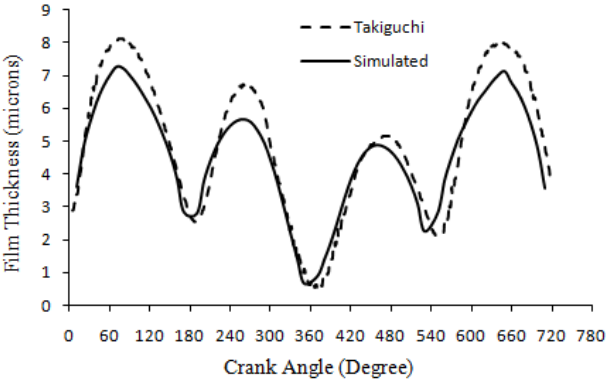

Fig. 13. Comparison of film thickness.

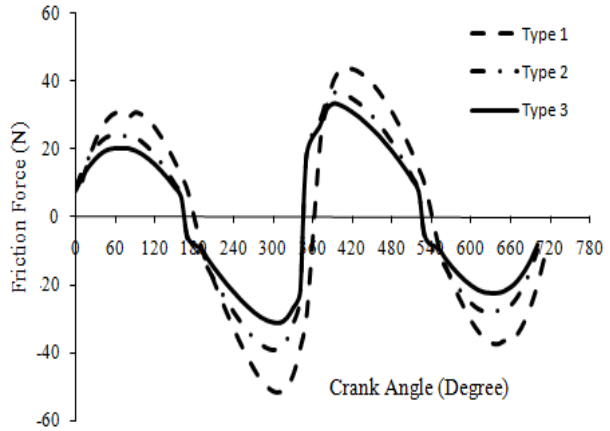

Fig. 14. Friction force.

Figure 14 shows the friction force acting between the ring and the cylinder liner, it can be seen that friction is maximum at point of maximum cylinder pressure. It can be attributed to the fact that there is an increase in asperity contact near the top and bottom dead center due to the mixed lubrication regime, whereas hydrodynamic lubrication exists for most part of the stroke. The friction was found maximum for type 1 ring profile, on the other hand type 3 has minimum friction force. At TDC the film thickness for type 3 profile is found to be lowest. It is expected that the friction due to lubricant viscosity was minimum which is in line with [14].

The total force acting between the ring and the liner is shown in figure 15, it comprises of the friction force acting because of the lubricant oil viscosity and the combustion mixture in the axial direction, and the ring elastic pressure force acting in radial direction. Type 3 ring designs has minimum total force acting on it, followed by type 2 with type 1 having the highest force acting on it at the TDC after compression.

From Fig. 16 friction coefficient was found minimum for type 3 rings, which is $1.82e^{-2}$ and it was found to be maximum for type 1 ring ($2.8e^{-2}$). The reason for minimum friction coefficient for type 3 ring was due to the minimum force acting between the ring and the cylinder liner. The total force can be reduced by using tribo-pads inserted into the piston and tribo-inserts inserted into the cylinder liner [16].

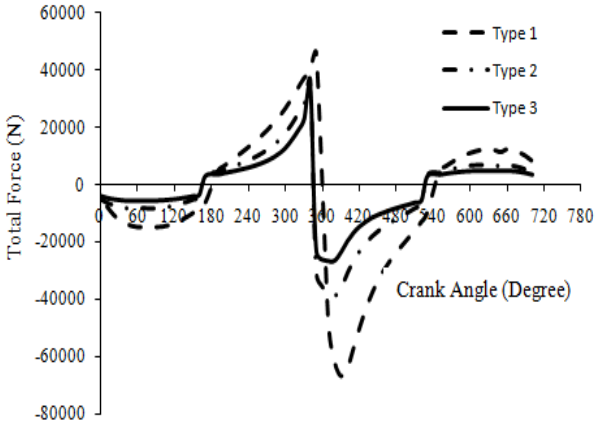

Fig. 14. Total force.

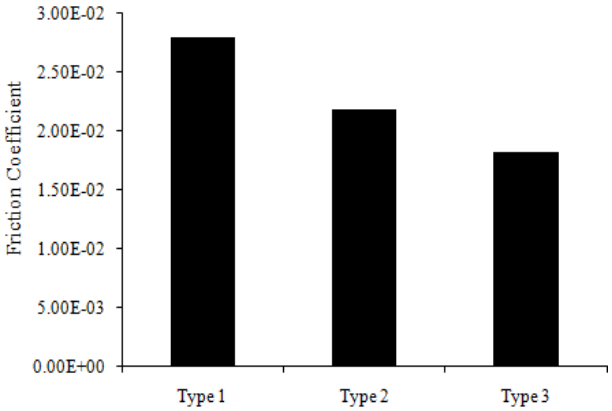

Fig. 16. Friction coefficient.

Type 3 ring profiles were then manufactured and the original compression ring was replaced by type 3 ring profile in the engine piston. Experiments were performed on the engine using motored floating liner method. Figure 17 and 18 shows the friction force acting on the liner. From the experimental result it can be seen that with the increase in speed, the friction force reduces, because of the increase in film thickness and better lubrication. On the other hand, as it was assumed to be hydrodynamic lubrication, the friction force obtained through simulation increases with the increase in speed. A high friction force was observed for simulated curve during power stroke. This is attributed to the fact that the engine was motored during experiments and no combustion took place, as a result the friction force during power stroke is less. The difference in the force during the combustion period was found to be 156.23 N and 267.72 N for 1500 rpm and 2000 rpm respectively. The force was calculated by subtracting the area under the curve of friction force acquired from the tests from the simulated friction force.

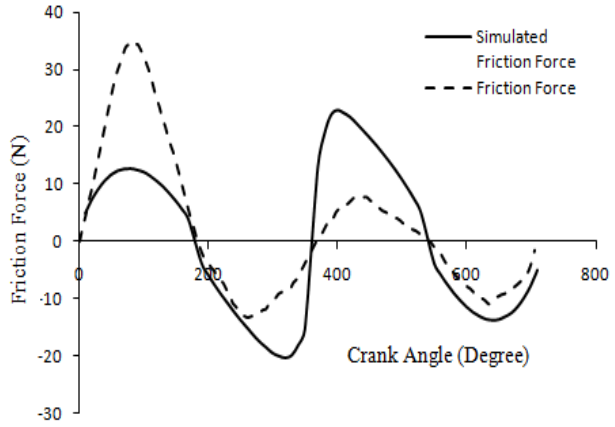

Fig. 17. Friction force at 1500 rpm.

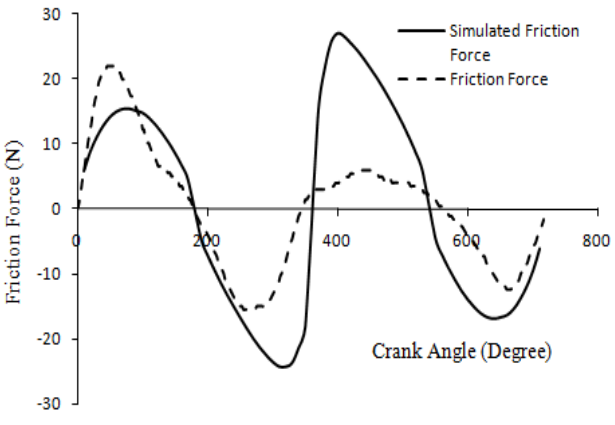

Fig. 18. Friction force at 2000 rpm.

5. CONCLUSION

In this study a ring dynamics model was simulated for the analysis of ring film thickness, the ring twist angles, the friction force and the friction coefficient using Secant method, for the compression ring. Three different ring profiles were chosen for the analysis purpose. Results indicate that hydrodynamic lubrication occurs for most part of the stroke except at the dead center where mixed lubrication regime was found due to reduced film thickness resulting in increased friction force.

Type 3 ring profiles was found to have the lowest friction coefficient and the lowest friction force, this would result in increase in fuel economy since the work done by the engine against the friction force would be reduced. On the other hand the oil film thickness was found to be minimum for type 3 profile, this could be a cause for concern since there can be direct contact between the ring and the cylinder liner thus increasing the wear rate of the liner.

Type 3 ring profile was manufactured and experimental work was carried out on the engine using floating liner method. The result from the experiment and the simulation were found to have a similar trend. The oil film thickness was validated by comparing the output of the MATLAB code (using the same data as given in literature) with literature and it was found to be in situ. This shows that whenever a change in ring design is needed this model can be used before going for actual manufacturing of the ring, thus saving time and expenses involved in ring manufacturing.

Further improvements can be done in this model by taking into consideration blow-by and finding its effect on hydrocarbon emissions and also finding the ring movement in the piston groove.

REFERENCES

[1] Y. Wakuri, M. Soejima, Y. Ejima, T. Hamatake, T. Kitahara: *Studies on friction characteristics of reciprocating engine*, SAE 952471, 1995.

[2] R.C. Singh, R. Chaudhary, R.K. Pandey, S. Maji: *Experimental Studies for the role of piston rings' face profile on performance of a diesel engine fueled with diesel and jatropha based biodiesel*,

Journal of Scientific and Industrial Research, Vol. 71, pp. 57-62, 2012.

[3] Y. Wakuri, T. Hamatake, M. Soejima, T. Kitahara: *Piston ring friction in internal combustion engines*, Tribology International, Vol. 25, No. 5, pp. 299-308, 1992.

[4] K. Wannatong, S. Chanchaona, S. Sanitjai: *Simulation algorithm for piston ring dynamics,* Simulation Modelling Practice and Theory, Vol. 16, pp. 127–146, 2008.

[5] Bryan O'Rourke, Rudolf Stanglmaier, Donald Radford: *Development of a floating - liner engine for improving the mechanical efficiency of high performance engines*, SAE 2006-01-3636, 2006.

[6] Kwang-soo Kim, Thom Godward, Masaaki Takiguchi, & Shuma Aoki: *Part 2: The effects of lubricating oil film thickness distribution on gasoline engine piston friction,* SAE 2007-01-1247, 2007.

[7] Philipe Saad, Lloyd Kamo, Milad Mekari, Walter Bryzik, Victor Wong, Nicolas Dmitrichenko, Rudolf Mnatsakanov: *Modeling and measurement of tribological parameters between piston rings and liner in turbocharged diesel engine*, SAE 2007-01-1440, 2007.

[8] Y. Harigaya, M. Suzuki, M. Takiguchi: *Analysis of oil film thickness on a piston ring of diesel engine: effect of oil film temperature*, J. Eng. Gas Turbines Power Vol. 125, pp. 596–603, 2003.

[9] T. Eduardo, & F.E.B. Nigro: *Piston Ring Pack and Cylinder Wear Modeling*, SAE 2001-01-0572, 2001.

[10] T. Tian: *Modelling the performance of the piston ring-pack in internal combustion engines,* PhD Thesis, Massachusetts Institute of Technology, 1997.

[11] Sung-Woo Cho, Sang Min Choi, Choong-Sik Bae: *Frictional modes of barrel shaped piston rings under flooded condition,* Tribology International, Vol. 33, No. 8, pp. 545-551, 2000.

[12] C.T. Chang: *Piston Ring Friction*, Master of Science Thesis, Massachusetts Institute of Technology, 1982.

[13] H. Rahnejat, P.C. Mishra, P.D. King: *Tribology of the ring–bore conjunction subject to a mixed regime of lubrication,* Proc. IMechE, Part C: J. Mechanical Engineering Science, Vol. 223, pp. 987-998, 2009.

[14] V.D' Agostino, P. Maresca, A. Senatore: *Theoretical analysis for friction losses minimization in piston rings*, Proceedings of the International Conference on Tribology, Parma, Italy, 20-22.09.2006.

[15] A. Kolchin, V. Demidov: *Design of Automotive Engines*, MIR Publishers, Moscow, 1984.

[16] R. Pesic, A. Davinic, S. Veinovic: *Methods of tribological improves and testing of piston engines, compressors and pumps*, Tribology In Industry, Vol. 27, No. 1&2, pp. 38-47, 2005.

NOMENCLATURE

η	dynamic Viscosity of oil (Ns/m^2)
L_1	width of ring above profile crest (m)
ρ	ring density (kg/m^3)
L_2	width of ring below profile crest (m)
$\overline{\theta}$	constant of integration
ΔP	pressure difference across the ring (N/m^2)
$\overline{a}$	characteristic ring tilt angle
P_e	ring elastic pressure (N/m^2)
a	ring inclination angle (°)
R_{cyl}	cylinder bore radius (m)
a'	normalized ring tilt angle
R	crank radius (m)
a_o'	normalized maximum ring tilt angle
$\overline{U}$	normalized piston speed
Al	connecting rod length (m)
V	circumferential ring speed
B	ring radial width (m)
W	ring axial width (m)
$\overline{h}$	characteristic film height
x	axial coordinate between ring and wall
h	local film height (m)
Y	piston axial location (m)
h_p	ring profile height (m)
Z_1	transformed coordinate at the top edge of the ring
h_r	ring reference distance (m)
h_r'	normalized ring reference film height
Z_2	transformed coordinate at the bottom edge of the ring

APPENDIX I

The piston acceleration, speed and piston position is calculated using the below equations
Position of piston

$$Y = R\cos\theta + Al\cos\varphi - Al - R$$

Velocity of the piston

$$V = -\left(DthetaR\sin\theta + DphiAl\sin\varphi\right)$$

Acceleration of piston

$$A = -\left(DDthetaR\sin\theta + Dtheta^2 R\cos\theta + DDphiAl\sin\varphi + Dphi^2 Al\cos\varphi\right)$$

Where

$$\varphi = \sin^{-1}\frac{R\sin\theta}{Al}$$

$$Dtheta = \frac{Rpm}{9.54928}$$

$$Dphi = Dtheta\frac{R}{Al}\frac{\cos\theta}{\cos\varphi}$$

$$DDtheta = -\left(Dtheta^2 R\cos\theta - Dtheta^2 R\frac{\sin\theta}{\cos\varphi}Al\sin\varphi\right)$$

$$DDphi = DDtheta\frac{R}{Al}\frac{\cos\theta}{\cos\varphi} + \left(Dphi\right)^2\tan\varphi - Dtheta^2\frac{R}{Al}\frac{\sin\theta}{\cos\varphi}$$